

MINIMIZATION, CONSTRAINTS AND COMPOSITE BÉZIER SURFACES¹

Arie JACOBI²

Department of Software Engineering,
Sami Shamoon Academic College of Engineering,
Beer Sheva, Israel

E-mail: ariej@mscc.huji.ac.il



Shilo LIFSCHUTZ³

Department of Accounting,
Academic Center of Law and Business,
Ramat-Gan, Israel

E-mail: shilo@clb.ac.il



Abstract: *This paper presents a global method for approximation and/or construction of surfaces using constraints. The method is based on a min max problem which describes approximation and differential geometric characteristics, constrained in order to achieve desired geometrical effects. The numerical solution of the problem takes full advantage of the Finite-Elements method and of constrained optimization algorithms.*

Key words: *Bézier surface; Offset surface; Surface Fitting; Offset Surface; Approximate Conversion; surface approximation; Surface simplification; Variational Problem Formulation; Finite-Element Method (FEM); FEM's hp-method; Lagrange Multipliers Formulation*

1. Introduction

Approximation of surfaces and construction of offset surfaces has a variety of applications. For example:

- Approximation to a set of scattered points in three-dimensional space originated from scientific experiments, earth terrain description, or data from satellites
- Exchanging format of formal data. It is required in geometric modeling systems for free form surfaces, as they use different mathematical representations and different polynomial bases for curves and surface representation
- Conversion between non-polynomial representations (such as rational surfaces) to polynomial ones.

Additional motivations for approximation are the ability of merging curves and surfaces in order to reduce information or the construction of offset curves and surfaces which are needed in tool paths planning for numerical control machines and in construction of a thick surface that is used as the outer (or inner) surface of objects such as, a car, an airplane, or a mold.

Finite element methods are an essential tool for the approximation of a solution of a partial differential equation and are based on the weak variational formulation of boundary and initial value problems. The importance of this property is twofold:

- It provides the proper setting for the existence of a very irregular solution to differential equations.
- The solution appears in the integral of a quantity over a domain, which can be broken up into the sum of integrals over an arbitrary collection of almost disjoint sub-domains whose union is the original domain.

These properties allow analysis to be done locally on a typical sufficiently small sub-domain, so that polynomial functions of various degrees are adequate for representing the local behavior of the solution (see [27]). In order to arrive at a global approximation of a solution of a partial differential equation in the finite element method, their contributions of local approximation over individual elements are assembled together in a systematic way. This leads to schemes which are robust in appropriate norms and insensitive to distortions and singularities of the mesh.

Desirable Properties of an Approximation Surface

We consider the following properties for curve approximation and construction:

- *End Points Interpolation* - The approximation surface's end points should interpolate the approximated surface's end points.
- *End Directions Preservation* - The approximation surface's boundary curves' end tangents should have the same direction as the approximated surface's boundary curves' end tangents.
- *Parametric and Geometric Continuity* - Creation of a smooth approximation surfaces. There are cases where a higher parametric continuity degree (C^1 or C^2) between the approximation surface patches is needed. It is also possible to ensure geometric continuity of first degree (GC^1) between the approximation surface patches.

2. Previous Work

There are several approaches for approximation of curves, surfaces, or points in three-dimensional space. Among the early important works in this field for the approximate conversion of curves and surfaces as well as the construction of offset curves and offset surfaces, we would like to signify the works of [11,26] and [16]-[24]. Among the recent works there is the work of Weiss et al. [30], that attempts to provide practical solutions to overcome problems of irregular distribution of data points which are over topologically irregular domains. The Weiss et al. method includes algorithms to compute a good initial parametrization, a procedure for handling weakly defined control points, a shape dependent knot refinement, and a fitting strategy to maintain tight tolerances and smoothness simultaneously. Their method achieves a high accuracy relative to the published 'standard' solutions.

Borges and Pastva [9] deal with the problem of fitting a single Bézier curve segment to a set of ordered data so that the error is minimized in the total least squares sense. They developed an algorithm for applying the Gauss-Newton method to this problem with a direct method for evaluating the Jacobian based on implicitly differentiating a pseudo-inverse. Chen Guo-Dong and Wang Guo-Jin [10] consider simultaneous fitting of multiple curves and surfaces to 3D measured data captured as part of a reverse engineering process, where constraints exist between the parameters of the curves or surfaces. Enforcing such constraints may be necessary

- to produce models of sufficiently accurate tolerances for import into a CAD system, and

- to produce models which successfully reproduce regularities and symmetries required by engineering applications.

There are several works in the CAGD field that use Bernstein-Bézier finite elements in the context of approximation. One of the earliest works on actual approximate conversion is Bercovier and Jacobi [3, 4] and Luscher [25]. Examples of later works that use FEM in CAGD are hierarchical methods for linear spline approximation and construction of surface triangulations or quadrangulations by adaptively subdividing a surface to a form of tree. It is used in an approximation to a set of scattered points in three-dimensional space using hierarchical spline and surface approximation methods such as in [8], or for approximation over irregular domain as introduced in [5, 6, 7, 31]. An implementation of cubic tetrahedral Bernstein-Bézier finite elements and their application in the context of facial surgery simulation is presented in [28]

3. Our Approach and its Strategy

Our approach uses the combination of the finite element method with the Bernstein-Bézier representation, introducing a valuable finite element due to the many advantages of the Bernstein-Bézier shape functions [14]. It introduces the construction of surfaces given by piecewise definitions of their parameter range and allows surface editing, both in the direction of several (lower order) surfaces approximating a single given one, or, conversely replacing several by a single one. This approach exploits the *p-method* and the *h-method* in FEM in order to improve approximation. This is done by using elements of higher degrees to overcome areas that are difficult to approximate and by using elements with lower degrees for approximating the rest of surface for implementing the *p-method*. For the implementation the *h-method* we use element mesh which is refined to increase accuracy. In order to achieve desired geometrical properties for the approximation surface, we incorporate parametric (C^0 - C^2) and geometric (GC^1) continuity constraints between the approximation surface patches, and other constraints, such as a constraint for the interpolation of the approximation surface end points with the end points of the given surface, or, a constraint to enforce the directions of the end edges of each boundary curve control polygon of the approximation surface to have the same directions as the tangents at the end points of the approximated surface boundary curves.

The strategy we use (see [3, 4]) is a global and continuous method for the approximation and construction of parametric surfaces. The method is based on a variational formulation which includes geometrical relations between surfaces and constraints upon the geometry and/or parameterization of the approximation surface. The variational formulation is based on the squared integrals of the zeroth, first, and second derivative (semi) norms of the approximation and approximated surfaces. We introduce the Lagrangian multiplier formulation for the constraints implementation. A weighting factor is related to each derivative (semi) norm. These weighting factors allow one to control the approximation of the related norm. The solution of this constrained variational problem is done by the Finite Element Method (FEM) over Bernstein basis functions.

Outline of this Paper

Description of the unconstrained problem, the constrained problem and its solution, is presented in sections 2-4. In section 5, a survey of the methods for estimating the approximation errors is given. Section 6, introduces the constraints we use to improve the approximation. A number of examples involving constraints, for surface degree reduction, surface merging and construction of offset surfaces are shown in section 7.

4. The Problem

Problem Statement

We will first define the problem without constraints. Given a parametric surface:
 $\mathbf{f}(u, v) = \mathbf{f}(f_1(u, v), f_2(u, v), f_3(u, v)), \quad u \in [a, b], v \in [c, d],$

find the unknown vector function

$\mathbf{x}(u, v) = \mathbf{x}(x_1(u, v), x_2(u, v), x_3(u, v)), \quad u \in [a, b], v \in [c, d],$

which is the solution by minimization, of one of the following three related problems we consider in this article:

$$\text{problem 1: } J^0(\mathbf{x}) = E(\mathbf{x}), \quad (1)$$

$$\text{problem 2: } J^1(\mathbf{x}) = E(\mathbf{x}) + \bar{E}(\mathbf{x}) \quad \text{and} \quad (2)$$

$$\text{problem 3: } J^2(\mathbf{x}) = E(\mathbf{x}) + \bar{E}(\mathbf{x}) + \hat{E}(\mathbf{x}), \quad (3)$$

where

$$E(x) = \alpha \iint_{\Omega} (\mathbf{x}(u, v) - \mathbf{f}(u, v))^2 \, dudv, \quad (4)$$

$$\bar{E}(x) = \beta \iint_{\Omega} \left(\frac{\partial}{\partial u} \mathbf{x}(u, v) - \frac{\partial}{\partial u} \mathbf{f}(u, v) \right)^2 + \left(\frac{\partial}{\partial v} \mathbf{x}(u, v) - \frac{\partial}{\partial v} \mathbf{f}(u, v) \right)^2 \, dudv, \quad (5)$$

and

$$\hat{E}(x) = \gamma \iint_{\Omega} \left(\frac{\partial^2}{\partial u^2} \mathbf{x}(u, v) - \frac{\partial^2}{\partial u^2} \mathbf{f}(u, v) \right)^2 + \left(\frac{\partial^2}{\partial v^2} \mathbf{x}(u, v) - \frac{\partial^2}{\partial v^2} \mathbf{f}(u, v) \right)^2 + \left(\frac{\partial^2}{\partial u \partial v} \mathbf{x}(u, v) - \frac{\partial^2}{\partial u \partial v} \mathbf{f}(u, v) \right)^2 \, dudv, \quad (6)$$

are the zeroth, first, and second error (semi) norms, respectively, and α , β , and γ positive moduli which are used as weighting factors.

Solution for the Problem Using the FEM Technique

In the following section we present the solution of the problem stated in section 2.1 using the FEM technique. The solution process includes: the partition of the problem's domain into two-dimensional elements, the calculation of a stiffness matrix \mathbf{M}_e and load vector \mathbf{m}_e for a given element e , the assembly of the elements' stiffness matrices and load vectors into the main stiffness matrix and load vector, and the calculation of the approximation error. The solution to one of the problems (1-3), follows the Galerkin-Ritz solution scheme (a computational example for the Rayleigh-Ritz and Galerkin methods, using the strong form of Poisson's equation can be seen in [29]).

The Approximation FEM Space

Given the partition:

$$a = u_0 < u_1 < u_2 \cdots < u_m = b$$

$$c = v_0 < v_1 < v_2 \cdots < v_n = d, \quad (7)$$

of the rectangular range

$$\bar{\Omega} = [a \leq u \leq b ; c \leq v \leq d], \quad (8)$$

each sub-range

$$\Delta_e = [u_i \leq u \leq u_{i+1} ; v_j \leq v \leq v_{j+1}] \quad (9)$$

for $i = 0, \dots, m - 1, j = 0, \dots, n - 1$ is the global parameter range of an element e , where $e = 0, \dots, L - 1$ and L is the number of elements.

We use the following linear transformation to establish the relation between the global parameters $u, v \in \Delta_e$ and the local parameters $r, s \in [0, 1]$:

$$\begin{bmatrix} u \\ v \end{bmatrix} = \begin{bmatrix} u_i \\ v_j \end{bmatrix} + ra + sb, \quad (10)$$

where

$$\mathbf{a} = \begin{bmatrix} u_{i+1} \\ v_j \end{bmatrix} - \begin{bmatrix} u_i \\ v_j \end{bmatrix}, \quad \text{and} \quad \mathbf{b} = \begin{bmatrix} u_i \\ v_{j+1} \end{bmatrix} - \begin{bmatrix} u_i \\ v_j \end{bmatrix}. \quad (11)$$

We introduce an $n \times m$ dimensional approximation space $V^{l,m,n}$, consisting of functions which are piecewise C^0 Bézier patches over the range $\bar{\Omega}$. Let

$$V^{l,m,n} = \{ \mathbf{x}(u, v) : \mathbf{x}(a, c) = \mathbf{f}(a, c), \quad \mathbf{x}(b, c) = \mathbf{f}(b, c), \\ \mathbf{x}(a, d) = \mathbf{f}(a, d), \quad \mathbf{x}(b, d) = \mathbf{f}(b, d) \}$$

such that there are

$$p \leq m \text{ and } q \leq n \text{ with}$$

$$\mathbf{x}(u, v) |_{\Delta_e} = \mathbf{S}_{p,q}(r(u), s(v))$$

a Bézier patch, for all $0 \leq e \leq L - 1$

$r(u), s(v)$ derived from equation (??),

$$\mathbf{x}(u, v) \in C^{l-1}([a, b]) \quad l = 0, 1, 2, 3, \text{ and}$$

C^{-1} is the space of functions

with discontinuities at u_e , or v_e only}. (12)

We define

$$V^l \equiv \bigcup_{m,n=1}^{\infty} V^{l,m,n}, \quad (13)$$

to be the minimization space, where $V^{l,m,n}$ is the finite-dimensional subspace (12) of V^l .

Problem Description for a given element e

Using partition (7) and given element e , where $e = 0, \dots, L - 1$ and L is the number of elements, we set:

$$E_e(\mathbf{x}) = \alpha \iint_{\Delta_e} (\mathbf{x}(u, v) - \mathbf{f}(u, v))^2 dudv, \quad (14)$$

$$\bar{E}_e(\mathbf{x}) = \beta \iint_{\Delta_e} \left(\frac{\partial}{\partial u} \mathbf{x}(u, v) - \frac{\partial}{\partial u} \mathbf{f}(u, v) \right)^2 + \left(\frac{\partial}{\partial v} \mathbf{x}(u, v) - \frac{\partial}{\partial v} \mathbf{f}(u, v) \right)^2 dudv, \quad (15)$$

and

$$\hat{E}_e(\mathbf{x}) = \gamma \iint_{\Delta_e} \left(\frac{\partial^2}{\partial u^2} \mathbf{x}(u, v) - \frac{\partial^2}{\partial u^2} \mathbf{f}(u, v) \right)^2 + \left(\frac{\partial^2}{\partial v^2} \mathbf{x}(u, v) - \frac{\partial^2}{\partial v^2} \mathbf{f}(u, v) \right)^2 + \left(\frac{\partial^2}{\partial u \partial v} \mathbf{x}(u, v) - \frac{\partial^2}{\partial u \partial v} \mathbf{f}(u, v) \right)^2 dudv, \quad (16)$$

to be the zeroth, first, and second error (semi) norms for the element e , and for the element sub-range Δ_e (as in (9)), respectively.

Let

$$J^l(\mathbf{x}(u, v)) = \sum_{e=0}^{L-1} J_e^l(\mathbf{x}(u, v)), \quad (17)$$

where

$$J_e^l(\mathbf{x}(u, v)) = J^l(\mathbf{x}(u, v)) |_{u,v \in \Delta_e}, \quad (18)$$

or,

$$J_e^l(\mathbf{x}(u, v)) = \left\{ \frac{1}{2} \mathbf{b}_e^T \mathbf{M}_e \mathbf{b}_e - \mathbf{m}_e^T \mathbf{b}_e \right\} \quad \text{for } 0 \leq e \leq L-1, \quad (19)$$

where for the e -th element,

$$\mathbf{b}_e \equiv [\mathbf{b}_{e0,0}, \dots, \mathbf{b}_{e,m,n}]^T,$$

is the vector of the unknown Bézier points, \mathbf{m}_e is the **element load vector** and \mathbf{M}_e is the **element stiffness matrix**.

Our objective is to find for all m, n the function $\mathbf{x}(u, v)$ which is taken over the space $V^{l,m,n}$, in order to approximate $\mathbf{f}(u, v)$ in some sense to be defined later.

General Solution of the Problem

After integration element by element, we obtain:

$$\sum_{e=0}^{L-1} J_e^l(\mathbf{x}_e) = \left\{ \frac{1}{2} \mathbf{b}^T \mathbf{M}^l \mathbf{b} - \mathbf{m}^{lT} \mathbf{b} \right\} \quad \text{for } l=0,1,2, \quad (20)$$

or

$$J^l(\mathbf{x}) = \left\{ \frac{1}{2} \mathbf{b}^T \mathbf{M} \mathbf{b} - \mathbf{m}^T \mathbf{b} \right\} \quad \text{for } l=0,1,2. \quad (21)$$

The elements' stiffness matrices \mathbf{M}_e^l , and load vectors \mathbf{m}_e^l , ($e = 0, \dots, L-1$), are assembled into the global stiffness matrix \mathbf{M} and load vector \mathbf{m} .

The minimum of each $J^l(\mathbf{x})$ in (21), is given by the approximation surface $\mathbf{x}(u, v)$, where \mathbf{b} is the solution of the system

$$\nabla_{\mathbf{b}} J^l(\mathbf{x}) = \mathbf{M} \mathbf{b} + \mathbf{m} = \vec{0}. \quad (22)$$

The system (22) is linear symmetric positive definite, and we use the LDL^T algorithm or the Conjugate-Gradient [32] to solve it. The coordinate components of $J^l(\mathbf{x})$ are decoupled, and the solution of the system refers to each coordinate component by itself.

Properties of the Global Stiffness Matrix

The global stiffness matrix is sparse, square banded, symmetric and positive definite. All of its elements are positive, the largest element per row or column is in the main diagonal, and the sum of all elements in a row (or in a column), is constant for each n . Its graph's shape is determined by the numbering of each of the degrees of freedom involved in the problem.

Let,

- $s = 3L(m+1)(n+1)$ be the sum of degrees of freedom for all the elements,
- ElementsAlongU, ElementsAlongV be the number of elements along u and v parameter lines respectively,
- and NodesAlongU, NodesAlongV be the number of nodes along u and v parameter lines respectively (every node contains 3 degrees of freedom).

For each element of degrees $m \times n$, there are $3(m + 1)(n + 1)$ degrees of freedom. Every boundary curve which shares two neighboring elements (patches) decreases the total number of degrees of freedom by:

$$s_b = \text{NodesAlong}U * (\text{ElementsAlong}V - 1) + \text{NodesAlong}V * (\text{ElementsAlong}U - 1).$$

Every cross section of such two boundary curves (meaning, at a cross section of four neighboring elements) decreases the total number of degrees of freedom by 9. The total sum of degrees of freedom at the cross sections is:

$$s_c = (\text{ElementsAlong}V - 1) * (\text{ElementsAlong}U - 1).$$

Therefore, the total number of the problem's degrees of freedom and the order of the global stiffness matrix is at most $s - s_b - s_c$. The creation of the global stiffness matrix is fast and efficient, since it involves only the assembly of the element stiffness matrices, which are pre-calculated and small.

The constrained Problem and its solution

Among the exiting numerous algorithms for solving a constrained optimization problem, some solve the constrained problem by replacing it with a family of unconstrained optimization problems. We use the Lagrangian multiplier formulation that converts the constrained minimization problem,

minimize $J^l(\mathbf{x})$ subject to the constraints $\varphi_i(\mathbf{x}) = 0, 1 \leq i \leq m$,
into the following unconstrained min max problem,

$$L_{\min \mathbf{x}, \max \lambda}^\Phi(\mathbf{x}, \lambda) = J^l(\mathbf{x}) + \sum_{i=1}^m \lambda_i \varphi_i(\mathbf{x}), \quad (23)$$

where

$$\lambda \equiv [\lambda_1, \dots, \lambda_m]^T. \quad (24)$$

λ_i is called the Lagrange multiplier for the constraint $\varphi_i(\mathbf{x}) = 0$. Solution of problem (23) with regard to the degrees of freedom in \mathbf{b} and λ yields the following necessary conditions:

$$\nabla L^\Phi(\mathbf{x}, \lambda) = \begin{cases} M\mathbf{b} - \mathbf{m} + \frac{\partial \sum_{i=1}^m \lambda_i \varphi_i(\mathbf{x})}{\partial \mathbf{b}} = \vec{0} \\ \sum_{i=1}^m \varphi_i(\mathbf{x}) = 0. \end{cases} \quad (25)$$

Error Estimation

Since the approximation depends on the parametrization of $\mathbf{x}(u, v)$ and $\mathbf{f}(u, v)$, it does not necessarily yield orthogonal error vectors between corresponding values of parameters. The absolute Euclidean minimum (or maximum) is at the point where two normals are collinear. Therefore a re-parametrization is needed so that the correction of the parametrization will direct the error vectors to be as orthogonal as possible to the tangent plane of \mathbf{x} at (u, v) . This will result in a better error estimation [16].

We use two types of discrete error estimators:

- the largest error Euclidean distance δ :
$$\delta = \max\{\| \mathbf{x}(u_i, v_j) - \mathbf{f}(u_i, v_j) \|\}, \quad u_i \in [a, b], \quad v_j \in [c, d]\}. \quad (26)$$

- the maximal angle deviation ϑ , between the normals:

$$\vartheta = \max \left\{ \arccos \left(\frac{\mathbf{n}_x(u_i, v_j) \cdot \mathbf{n}_f(u_i, v_j)}{\| \mathbf{n}_x(u_i, v_j) \| \| \mathbf{n}_f(u_i, v_j) \|} \right), \quad u_i \in [a, b], \quad v_j \in [c, d] \right\}. \quad (27)$$

In order to use error measurements which are not dependent on the parametrization, we use the zeroth, first and second derivative error (semi) norms (4-6) for error estimation. The zero derivative error norm (squared error integral) is the L^2 norm. The first and second derivative error (semi) norms are used to estimate the error in the first and second partial derivatives displacements.

We also use the error (semi) norms $E(x)/S^2$, $\bar{E}(x)/S^2$ and $\hat{E}(x)/S^2$, which measure the mean error displacement per unit area, where S is an approximated area of $f(u)$. For error in curvature, we use the Gaussian curvature L^2 error norm:

$$E^K = \int_a^b \int_c^d (\tilde{K} - K)^2 dudv, \quad (28)$$

where \tilde{K} is the Gaussian curvature of the approximated surface $\mathbf{x}(u, v)$, and the Gaussian curvature mean deviation error:

$$E_m^K = \frac{\int_a^b \int_c^d (\tilde{K} - K)^2 dudv}{\int_a^b \int_c^d (K)^2 dudv}. \quad (29)$$

We also use the mean curvature L^2 error norm:

$$E^H = \int_a^b \int_c^d (\tilde{H} - H)^2 dudv \quad (30)$$

where \tilde{H} is the mean curvature of the approximated surface $\mathbf{x}(u, v)$, and the mean curvature mean deviation error:

$$E_m^H = \frac{\int_a^b \int_c^d (\tilde{H} - H)^2 dudv}{\int_a^b \int_c^d (H)^2 dudv}. \quad (31)$$

Error estimations of all types presented in this section are presented in tables 1-2, for the approximation of a Bézier patch of degrees 5 x 3, with sizes of 3 x 28.5 mm and approximated area of $S = 85.36 \text{ mm}^2$ (see Figure 1), by a Bézier patch with different degrees and continuity orders between elements.

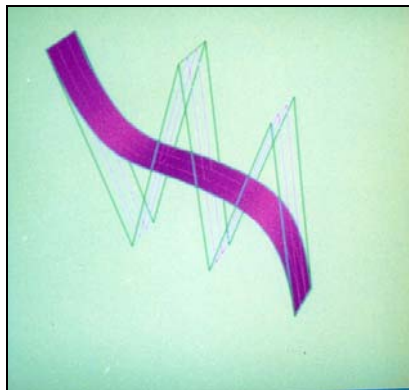
degrees	segments	δ	ϑ	$E(x)/S^2$	$\bar{E}(x)/S^2$	$\hat{E}(x)/S^2$
2 x 3	1 x 1	1.479	0.348	2.348264e-04	2.523826e-05	5.107362e-05
3 x 3	1 x 1	0.380	0.240	1.465209e-05	1.818131e-06	5.128979e-05
4 x 3	1 x 1	0.365	0.220	1.395186e-05	1.595004e-06	1.254311e-05
5 x 3	1 x 1	0.0	1.13e-07	4.447024e-19	2.911940e-18	1.115636e-04
3 x 3	2 x 1	0.450	0.245	1.396280e-05	2.934349e-06	1.763063e-04
4 x 3	2 x 1	0.041	0.039	1.395732e-07	7.531847e-08	1.712148e-04
2 x 3	3 x 1	0.540	0.276	1.530292e-05	2.978221e-06	1.713536e-04
3 x 3	3 x 1	0.051	0.058	1.651474e-07	1.487066e-07	1.769908e-04

4 x 3	3 x 1	0.002	0.006	5.137242e-10	2.253008e-09	1.929809e-04
4 x 3	3 x 1	0.002	0.005	4.885186e-10	1.619946e-09	1.930424e-04
4 x 3	3 x 1	0.011	0.001	8.110637e-09	8.997212e-09	1.935975e-04

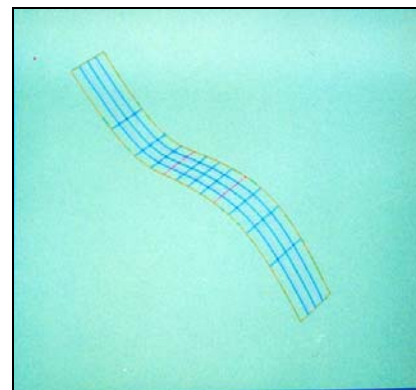
Table 1: Various error estimations by the derivative error (semi) norms, for the approximation of a Bézier patch of degrees 5 x 3, with sizes of 3 x 28.5 mm and approximated area of $S = 85.36 \text{ mm}^2$, by a Bézier patch with different degrees. See Figure: 1

degrees	E^K	E_m^K	E^H	E_m^H
2 x 3	3.339768e+00	9.764867e-01	5.592338e+00	8.735588e-01
3 x 3	2.059826e+00	5.233216e-01	3.087451e-01	5.079714e-02
4 x 3	6.194731e-01	1.573840e-01	2.562805e-01	4.216526e-02
5 x 3	2.012408e-14	5.084107e-15	1.561175e-14	2.442805e-15
3 x 3	8.055888e-01	3.363193e-01	3.795821e-01	5.976159e-02
4 x 3	8.473989e+00	3.537743e+00	8.030403e-02	1.264311e-02
2 x 3	4.354274e-01	5.014103e-01	4.724982e-01	7.439097e-02
3 x 3	1.259487e+01	1.449829e+01	1.270752e-01	1.998752e-02
4 x 3	8.319730e+01	9.577063e+01	6.819476e-01	1.072628e-01
4 x 3	8.309422e+01	9.565197e+01	6.816075e-01	1.072093e-01
4 x 3	8.281638e+01	9.533215e+01	6.837922e-01	1.075529e-01

Table 2: Various error estimations by the curvature error norms, for the same given Bézier patch and approximation surfaces as in Table 1.



(a) Given surface



(b) The approximation surface.

Figure 1: Reduction of a Bézier patch of degrees (5 x 3), with sizes of 3 x 28.5 mm and approximated area of $S = 85.36 \text{ mm}^2$, by an approximation (C^2, C^3) Bézier surface with three patches of degrees (4 x 3).

5. Incorporation of Constraints

In this section we introduce the description and implementation of constraints which are imposed upon the approximation or the construction of surfaces in order to achieve the following desired geometrical effects:

Constraints for Surface's End Points Interpolation

In order to create a better approximation, the end points of the approximation surface should interpolate the end points of the given surface. Meaning, the conditions: $\mathbf{x}(a, c) = \mathbf{f}(a, c)$, $\mathbf{x}(b, c) = \mathbf{f}(b, c)$, $\mathbf{x}(a, c) = \mathbf{f}(a, c)$, and $\mathbf{x}(b, c) = \mathbf{f}(b, c)$, (32) must be satisfied.

First Derivative Interpolation at the End Points of Boundary Curves

The direction of the end edges of each boundary curve control polygon of the approximation surface, are constrained to have the same directions as the tangents at the end points of the approximated surface boundary curves. The method used for this constraint, is the same one used for curves, as described in [4].

Constraints for C^k , Continuity Between Elements

Higher continuity between elements will not necessarily improve the approximation but will create a smoother approximation surface, a feature which is desirable in many cases, such as, the design of mechanical parts which requires first- or second- order smoothness, or in the definition of a tool path for NC machine where we need the speed and the acceleration of the tool to be continuous. This can be achieved by C^1 and C^2 parametric continuity.

A Bézier surface may contain several patches joined together with a given continuity. Let $\mathbf{x}^{m,n}(u, v)$ and $\mathbf{y}^{m,n}(u, v)$ be two Bézier patches defined over $[u_{i-1}, u_i] \times [v_{j-1}, v_j]$ and $[u_i, u_i + 1] \times [v_{j-1}, v_j]$ respectively. $\mathbf{x}^{m,n}$ and $\mathbf{y}^{m,n}$ have C^q continuity along the parametric line $u = u_i$, if

$$\frac{\partial^q}{\partial u^q} \mathbf{x}^{m,n}(u_i, v) = \frac{\partial^q}{\partial u^q} \mathbf{y}^{m,n}(u_i, v). \quad (33)$$

For Bézier surfaces it is possible to reduce the surface problem to several curve problems. Using the *cross boundary derivative* (the derivative at the common boundary curve) with respect to the global parameters u, v we obtain:

$$\frac{1}{(\Delta_{i-1})^q} \sum_{j=0}^n \Delta^{q,0} \mathbf{b}_{m-q,j} B_j^n(v) = \frac{1}{(\Delta_i)^q} \sum_{j=0}^n \Delta^{q,0} \mathbf{b}_{m,j} B_j^n(v). \quad (34)$$

It follows that along the parametric line $u = u_i$,

$$\frac{1}{(\Delta_{i-1})^q} \Delta^{q,0} \mathbf{b}_{m-q,j} = \frac{1}{(\Delta_i)^q} \Delta^{q,0} \mathbf{b}_{m,j} \quad j = 0, \dots, n. \quad (35)$$

Equations (35) are conditions on rows of control points across the boundary curve which represents C^q Bézier curves (see [14,23]).

The continuity constraints can be imposed only on part of the patches. This is usually done on a boundary of complete two rows or two columns in the mesh of elements. This way we construct a surface the in some parts it has a high continuity degree (C^2 for example), and in other parts a C^0 continuity is left to produce a corner or a cusp.

Examples

Approximation of surfaces can be used in the applications of: degree reduction of surfaces, merging of surfaces with large number of patches, and construction of offset

surfaces. Reduction of degree of high order polynomial surfaces to polynomials of a lower order. The degree reduction approximation might reduce or increase the number of surface patches. It is sometimes needed to merge a surface which is constructed from many small patches into a surface with less patches of the same degrees, or even with higher degrees. The construction of a parametric offset surface, is done by approximating the offset surface $x_d(u, v)$ to the given surface $f(u, v)$.

$$x_d(u, v) = f(u, v) + d\mathbf{n}(u, v), \quad (36)$$

where $\mathbf{n}(u, v)$ is the principal normal vector, and d is the offset distance along $\mathbf{n}(u, v)$.

Among the surfaces that we used in the section, there are the following three surfaces:

1. The surface BRODE (Fig. 2(a)), which is a 9 x 9 Bézier patch with sizes of 100 x 140 mm.
2. The surface SEITE1 (Fig. 2(b)), which is a collection of 9 x 7 Bézier patches, each of degrees 3 x 3 and sizes about 500 x 2200 mm.
3. The surface SURFB (Fig. 2(c)), which is a collection of 17 x 63 Bézier patches, each of degrees 5 x 5 and sizes about 450 x 1800 mm.

These surfaces were used as test examples (bench-mark) for the comparison between spline conversion methods (See for example, [12, 13, 15, 24]).

The bench-mark specifications were to convert these surfaces to a 3 x 3 or a 5 x 5 Bézier or B-Spline surface with a maximal error tolerance of 0.1 and 0.01 mm. For each of the surfaces involved in the bench-mark a table was presented, in which the degrees and the segment number of the result approximation surface are listed in the first two columns. In the third column the inner continuities in both parameter directions are entered. The fourth column contains the compression factor. The compression factor for the conversion to Bézier surface is given by the quotient:

$$\frac{\text{number of Bézier points of the given patches}}{\text{number of Bézier points of the converted patches}},$$

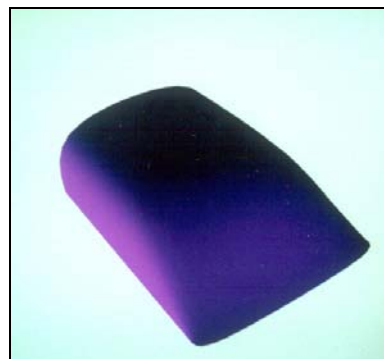
and the compression factor for the conversion to B-Spline surface is given by the quotient:

$$\frac{3(\text{number of Bézier points of the given patches})}{3(\text{number of B-Spline control points}) + \text{knots in the knot vectors}}.$$

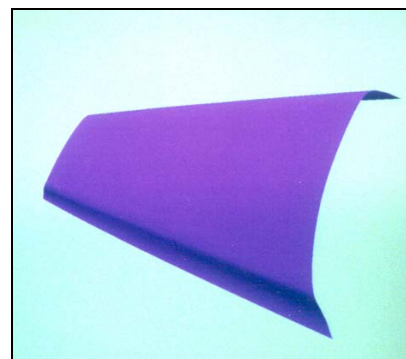
In the fifth column the approximation presents the prescribed approximation tolerance, and in the sixth column the largest error Euclidean distance

$$\delta = \max\{\|x(u_i, v_j) - f(u_i, v_j)\|, \quad u_i \in [a, b], \quad v_j \in [c, d]\},$$

is given. We will use the same format of table for our examples.



(a) The BRODE surface



(b) The SEITE1 surface



(c) The SURFB surface

Figure 2 : Benchmark Surfaces.

Constraints results

Examples of constrained approximations are introduced in our results of the benchmark surfaces BRODE, SEITE1 and SURFB in tables (3-5). These examples emphasize the *p-method* and *h-method* of FEM in the approximation. We see for example in table (5) that presents approximation results for the SURFB surface (Figure 2(c)), that each line in the table introduces an approximation with a different mesh size (signified by the segments column of the table) and patch degrees. One can see the different continuity degrees achieved by the imposing C^1 or C^2 continuity constraints between the approximation surface patches. The last two lines of table (3), represent an approximation of the BRODE surface (Figure 2(a)), that uses a mesh of elements of different degrees, attached with C^0 continuity. These results display how the combination of the *hp-methods* in FEM was used in the approximation scheme of this research.

Another example that displays an approximation of an offset surface is presented in figure (3). The approximation offset surface that approximated a surface of degrees (3 x 3) (Figure 3(a)), has an offset distance of -0.4 mm , two patches of degrees (3 x 3) and (C^1, C^3) continuity between its patches. The approximation integrates the end points and first derivative interpolation constraints.

All the above examples integrated the end points and first derivative interpolation constraints (see sections 6.1-6.2, respectively).

Table 3. surface: BRODE:

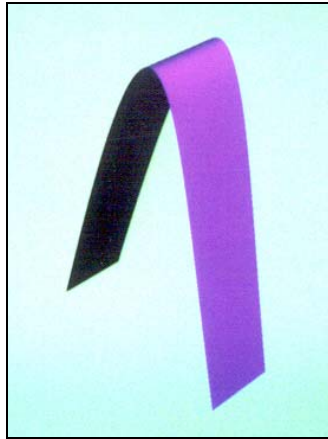
surface: BRODE: degree: 9 x 9, segments: 1 x 1					
degree	segments	minimal continuity	compression factor	error tolerance	measured error
3 x 3	5 x 3	C^2, C^2	0.42	0.01	0.008
	3 x 2	C^1, C^1	1.04	0.01	0.01
	2 x 2	C^1, C^1	1.56	0.1	0.042
	3 x 2	C^2, C^2	1.04	0.1	0.018
4 x 3	2 x 2	C^2, C^2	1.25	0.1	0.017
4 x 4	2 x 2	C^2, C^2	1.0	0.01	0.006
	2 x 1	C^2, C^2	2.0	0.1	0.026
4 x 5	2 x 1	C^2, C^2	1.66	0.1	0.016
5 x 3	1 x 2	C^2, C^2	2.08	0.1	0.023
5 x 5	2 x 2	C^2, C^2	0.69	0.01	0.002
	2 x 1	C^2, C^2	1.39	0.1	0.015
	1 x 1		2.78	0.1	0.022
7 x 6	1 x 1		1.79	0.1	0.004
7 x 7	1 x 1		1.56	0.1	0.001
3,5,3 x 3,4	3 x 2	C^0, C^0	1.04	0.01	0.008425
3,3,2,2,3,3 x 3,4	6 x 2	C^0, C^0	0.52	0.01	0.009057

Table 4. surface: SEIT1

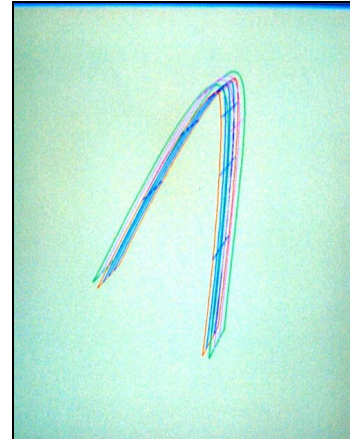
urface: SEITE1: degree: 3 x 3, segments: 9 x 7					
degree	segments	minimal continuity	compression factor	error tolerance	measured error
3 x 3	8 x 7	C^2, C^2	1.13	0.01	0.0088
	2 x 7	C^2, C^2	4.5	0.1	0.1
4 x 3	2 x 7	C^2, C^2	3.6	0.1	0.068960
5 x 3	3 x 7	C^2, C^2	2.0	0.01	0.003987
5 x 5	3 x 7	C^2, C^2	1.33	0.01	0.003985
	2 x 7	C^2, C^2	2.0	0.1	0.023714
	1 x 7	C^2, C^2	4.0	0.1	0.1

Table 5. surface: SURFB

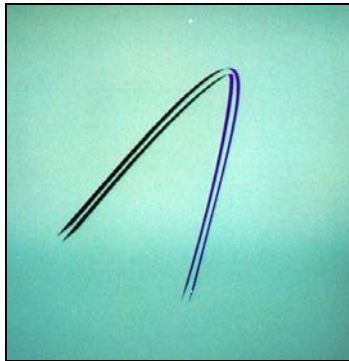
surface: SURFB: degree: 5 x 5, segments: 17 x 63					
degree	segments	minimal continuity	compression factor	error tolerance	measured error
3 x 3	17 x 29	C^2, C^2	4.89	0.01	0.008632
	17 x 16	C^2, C^2	8.86	0.1	0.076872
3 x 4	17 x 13	C^2, C^2	8.72	0.1	0.016416
3 x 5	17 x 13	C^2, C^2	7.27	0.01	0.004687
	17 x 8	C^2, C^2	11.81	0.1	0.041205
4 x 4	14 x 17	C^2, C^2	6.48	0.01	0.008888
	8 x 11	C^2, C^2	17.53	0.1	0.079889
5 x 4	6 x 11	C^2, C^2	19.47	0.1	0.095811
5 x 5	14 x 13	C^2, C^2	5.88	0.01	0.008055
	6 x 6	C^2, C^2	29.75	0.1	0.075385



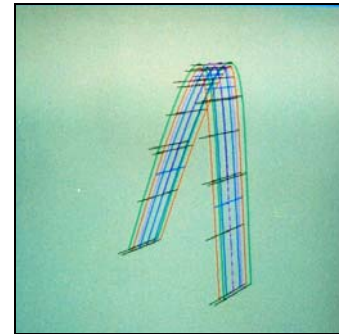
(a) Bézier patch of degrees



(b) The shaded surfaces



(c) The shaded surfaces



(d) The surfaces with drawing of the tangents along the v-parameter lines

Figure 3: An offset Bézier surface to the surface (a), with two patches of degrees 3×3 , (C^1, C^3) continuity between patches and offset length of -0.4 .

6. Conclusions and Future Work

In our work we introduced a global and continuous method for approximation and/or construction of surfaces. It is based on a minimization of a functional which makes use of global and continuous criteria (4-6), for approximation and construction. Constraints were integrated in the approximation to obtain some specific characteristics. Some of the properties we would like to obtain are aimed at improving the approximation, such as, end points interpolation and end direction preservation. Others are designed to impose a desirable form upon the approximation surface, for instance, parametric continuity between the approximation surface's patches. The constraints used were linear, equality, and operates on a discrete parameter range. We used the Lagrangian multiplier formulation for the constrained problem.

The numerical solution of the functional uses FEM with the Bernstein-Bézier representation for the shape functions, and presents cardinal advantages:

- The approximation method operates globally on the given problem's domain.
- Segmentation of the approximation surface is natural to FEM, because of the subdivision of a FEM problem's domain into elements.

- Every element is treated separately, and its "influence" is added to the general stiffness matrix such that there is no limitation on the form of the general range combined from a collection of elements.
- It is possible to approximate, using different elements with different degrees of elements (Bézier patches).
- The system of equations is linear for any degrees of the elements and any order of parametric continuity C^n between the elements.
- The use of Bézier-Bernstein representation grants good properties for the stiffness matrix, and saves much of the approximation calculation using proper solution methods (such LDL^T). Most of the calculation of the element matrices is prepared in advance and can be used regardless of the subdivision of problem's domain.
- There is not a pre-requirement on the given surface's continuity.
- It is possible to approximate, using different elements with different degrees of parametric continuity, including C^0 .

As the next step in this research, we intend to include different types of linear and nonlinear constraints, of equality and/or inequality types, on a discrete or a continuous parameter range. These constraints are aimed at improving the approximation, or at imposing a desirable form upon the approximation surface. Examples of such constraints are, optimal construction using reparametrization, opening loops for given looped surfaces, or avoiding loops in the approximation of offset surfaces.

References

1. Babuska, I., Szabo, B.A. and Katz, I.N. **The p-version of the Finite Element Method**, SIAM J. Numerical Analysis, No. 18, 1981, pp.515-545
2. Babuska, Ivo and Suri Manil **The P and H-P Versions of the Finite Element Method, Basic Principles and Properties**, SIAM Review, Vol. 36, No. 4, Dec. 1994, pp. 578-632
3. Bercovier Michel and Jacobi Arie **Approximation and/or Construction of Curves by Minimization Methods with or with-out Constraints**, MAN Mathematical Modelling and Numerical Analysis, Vol. 26, No. 1, 1992, pp.211-232
4. Bercovier Michel and Jacobi Arie **Minimization, Constraints and Composite Bézier Curves**, Computer Aided Geometric De-sign - Computer Aided Geometric Design, Vol: 11, 1994, pp. 533-563
5. Bercovier, M., Volpin, O. and Matskewich, T. **Globally G1 Free Form Surfaces using "Real" Plate Energy Invariant Energy Methods**, Curves and Surfaces with Applications in CAGD, 2, 1997
6. Matskewich, T., Volpin, O. and Bercovier, M. **Discrete G1 Assembly of patches over irregular meshes**, Proceedings of Curves and Surfaces in CAGD, Norway, 1997
7. O. Volpin and M. Bercovier **Generation of Quadrilateral meshes from triangular data with resulting smooth surface reconstruction**, Proc.IEEEConf.InformationVisualisation-IV98,London, 1998, online source: <http://www.computer.org/proceedings/IV/8509/>
8. Bercovier, M. and Volpin, O. **Hierarchical Bezier Surfacee over Arbitrary Meshes**, Computer Graphics Forum,18(4), 1999, pp. 223-236
9. Borges F.and Pastva T. **Total least squares fitting of Bézier and B-spline curves to ordered data**, Computer Aided Geometric Design, Vol. 19, No. 4, 2002, pp. 275-289
10. Chen Guo-Dong and Wang Guo-Jin **Optimal multi-degree reduction of Bézier curves with constraints of endpoints continuity**, Computer Aided Geometric Design, Vol. 19, No. 4, 2002, pp. 275-289
11. Dannenberg, L.; Nowacki, H. **Approximate Conversion of Surface Representations with Polynomials Bases**, Computer Aided Geometric Design, No. 2, 1985,

- pp. 123-132
12. Dokken, T. and Lyche, T. **Spline Conversion: Existing Solutions and Open Problems**, In: Laurent, P.J. and Méhauté A.L. and Schumaker L.L. Curves and Surfaces in Geometric Design, A K Peters, Wellesley, 1994, pp. 121-130
 13. Eck, M. and Hadenfeld, J. **A Stepwise Algorithm for Converting B-Splines**, In: Laurent, P.J. and Mehaute A.L. and Schumaker L.L. Curves and Surfaces in Geometric Design, A K Peters, Wellesley, 1994, 121-130
 14. Farin, G. **Curves and Surfaces for Computer Aided Geometric Design, A Practical Guide**, Academic Press, Inc., Boston, 3rd Ed, 1988
 15. Goult, R. J. **Applications of Constrained polynomials to Curve and Surface Approximation**, In: Laurent, P.J. and Mehaute A.L. and Schumaker L.L. Curves and Surfaces in Geometric Design, A K Peters, Wellesley, 1994, pp. 217-224
 16. Hoschek, J. **O set Curves in the Plane**, Computer Aided Design, No. 4, 1985, pp. 59-66
 17. Hoschek, J. **Approximation Conversion of Spline Curves**, Computer Aided Geometric Design, No. 17, 1987, pp. 77-82
 18. Hoschek, J. **Spline Approximation of O set Curves**, Computer Aided Geometric Design, Vol. 5, 1988, pp. 33-40
 19. Hoschek, J. **Intrinsic Parameterization for Approximation**, Computer Aided Geometric Design, Vol. 5, 1988, pp. 27-31
 20. Hoschek, J., Schneider, F. J. and Wassum, P. **Optimal Approximation Conversion of Spline Surfaces**, Computer Aided Design, No. 20, 1988, pp. 457-483
 21. Hoschek, J. and Wissel, N. **Optimal Approximate Conversion of Spline Curves and Spline Approximation of O set Curves**, Computer Aided Design, Vol. 20, No. 8, 1988, pp. 475-483
 22. Hoschek, J. and Schneider, F.J., Spline Conversion for Trimmed Rational Bézier- and B-Spline Surfaces, Computer Aided Design, Vol 22, No. 9 (1990), pp. 580-590.
 23. Hoschek, J. and Lasser, D. **Computer Aided Geometric design**, A K Pters, Wellesley, 1993
 24. Hoschek, J. and Schneider, F.J. **Approximate Conversion and Data Compression of Integral and Rational B-spline Surfaces**, In: Laurent, P.J. and Mehaute A.L. and Schumaker L.L. Curves and Surfaces in Geometric Design, A K Peters, Wellesley, 1994, pp. 241-250
 25. Luscher, N. **The Bernstein-Bézier Technique in the Finite Element Method, Exemplary for the Univariate Case**, Technical Report from the University of Braunschweig, 1988
 26. Nowacki, H., Dingyuan, L. and Xinmin, L. **Fairing Bézier Curves With Constraints**, Computer Aided Geometric Design, No. 7, 1990, pp. 43-55
 27. Oden J. Tinsley **Finite Elements: An Introduction**, In: Ciarlet P.G. and Lions J.L., editors, Handbook of Numerical Analysis. Finite Element Methods (Part 1), Vol. II, North-Holland, 1991
 28. Roth, S. H. M. **BernsteinBézier Representations for Facial Surgery Simulation**, A thesis dissertation submitted to the Swiss Federal Institute of Technology, ETH, Zurich, 2002
 29. Strang, G. **Introduction to Applied Mathematics**, Wellesley-Cambridge Press, 1986
 30. Weiss, V., Andorb, L., Rennera, G. and Veradya, T. **Advanced surface fitting techniques**, Computer Aided Geometric Design Vol. 19, No. 1, 2002, pp. 19-42
 31. Xiquan Shi, Tianjun Wang and Piqiang Yu **A practical construction of G1 smooth biquintic B-spline surfaces over arbitrary topology**, Computer-Aided Design, 36, (2004), 413424
 32. Zienkiewicz, O. C. **The Finite Element Method in Engineering Science**, McGraw-Hill, London, 1971

¹ Acknowledgments

This research was partially supported by a grant from the Ministry of Science and Culture, Land Hessen, W. Germany

² **Arie Jacobi** is Senior Lecturer in the Software Engineering Department, Sami Shamoon College of Engineering, Israel. He was born in Israel in 1956, and received his B.Sc., M.Sc. and Ph.D. degrees in Computer Science from the Hebrew University of Jerusalem, Israel. Dr. Jacobi's professional experience includes 28 years of engineering and management positions in Israeli software and high-tech industries. His current research interests are in Computer Aided Geometric Design and Approximation Theory, in which Dr. Jacobi investigate different numerical and geometrical methods for approximation and construction of curves and surfaces. Another field of research interest is Complexity in Social Networks. Dr. Jacobi is now investigating problems of trust for information, which is distributed over social networks whose growth and evolution are primarily driven by personal interactions. Dr. Jacobi has published in leading journals such as Computer Aided Geometric Design (CAGD) and Mathematical Modeling and Numerical Analysis (MAN).

³ **Shilo Lifschutz**, is the chairman of the accounting department and a faculty member of accounting and finance at the Academic Center of Law and Business, Ramat Gan, Israel. He holds a PhD from the Hebrew University of Jerusalem and is a CPA (Israel and Illinois, USA). His main research interests are quantitative methods in finance and risk management.